TECHNO-ECONOMIC ASSESSMENT OF WASTE HEAT RECOVERY FOR GREEN HYDROGEN PRODUCTION: A SIMULATION STUDY

Natalie FRASSL (*), Nina RANJBAR-SISTANI, Yannick WIMMER, Judith KAPELLER, Klara MAGGAUER, Johannes KATHAN

Austrian Institute of Technology; Giefinggasse 2, 1210 Wien; natalie.frassl@ait.ac.at; www.ait.ac.at

Abstract: The demand for hydrogen as a green energy carrier grows as energy sources are shifting towards sustainable solutions. Alkaline electrolysers are a clean path to provide hydrogen, but with an efficiency of 60 to 80 % a significant portion of the electricity input is lost. Therefore, there is considerable interest in increasing an electrolyser's overall efficiency by waste heat recovery. This study investigates the technical and economic prospects of harnessing waste heat from an alkaline electrolyser powered by surplus renewable energy and using it as a feed-in source for a district heating system. Utilizing an existing simulation framework for renewable power plants, this work integrates an electrolyser model, which is validated against established literature. The analysis focuses on the impact of heat extraction and of heat sales on system efficiency, economic viability and hydrogen pricing. Findings reveal enhanced efficiency with heat supply, particularly for smaller electrolyser configurations with an improvement of around 10.5 percentage points. The Levelized Cost of Hydrogen (LCOH) is only minimally reduced by heat sales and varies greatly with electrolyser and renewable capacity. These estimated LCOH values range from 1.3 to 2.6 €/kg and can rival non-sustainable hydrogen prices given certain conditions, due to assuming cost-free surplus electricity in this study. Findings further show viable heat sales for the more ideal smaller electrolyser sizes. Concurrently, the necessity of a more complex cooling strategy is revealed to better evaluate larger systems. Overall, results highlight the potential of synergizing electrolysis with district heating, providing valuable insights for the integration of renewable-powered electrolysis into future energy systems.

Keywords: Alkaline Electrolysis, Waste Heat Recovery, Techno-Economic Analysis, Renewable Hydrogen, Modelling of Electrolyser System

1 Introduction

1.1 Background

The fluctuating nature of renewable energy generation poses a challenge worldwide in the fight against fossil fuel energy sources. Hydrogen as a future energy carrier represents a possible solution by utilising and storing excess electric energy in times of abundance. It can be used in various sectors like transport, industrial processes, heat and electricity production and consequently, sustainable hydrogen is essential for a decarbonized, integrated and connected energy system of the future [4, 6, 22].

In 2020, the EU has released their Hydrogen Strategy, which includes the goal of implementing a minimum of 40 GW electrolysers for green hydrogen production until 2030. Up to 10 million tons of H_2 are targeted to be manufactured, but substantial hydrogen production also comes with an undisputed drawback [4, 9].

Electrolysis, the process of splitting water into hydrogen and oxygen without direct carbon emissions, has considerable energy losses. Alkaline water electrolysis (AEL), currently the most mature technology, has an efficiency of about 60-80 % regarding the higher heating value (HHV) of hydrogen, while the majority of the rest electricity input is transformed to heat and usually lost to the environment [6, 16].

As electrolyser capacities rise, there is a growing interest in utilizing their considerable excess heat and increasing the overall efficiency of the system. Waste heat generated by electrolysers has the potential to supply heat to a diverse number of applications like low-temperature industry processes, heating of buildings or district heating networks [22].

1.2 Purpose

This thesis aims to analyse the potential of utilizing waste heat from an alkaline electrolyser for the supply of a district heating network. The studied system consists of a wind park and various photovoltaic capacities that supply excess electrical energy to an electrolyser. Subsequent to a system simulation, a techno-economic assessment of this project focusing on the effects of re-using generated heat on system efficiency and Levelized Cost of Hydrogen (LCOH) is conducted. Additionally, the process of selling heat is checked for viability.

In order to be able to closely investigate the plant, a previously developed, python-based simulation tool for renewable power plants is used, for which an AEL-Model is developed and integrated.

1.3 Delimitations

Within the analysed system, a storage component of either hydrogen or heat is not examined as well as a heat pump for an elevated output temperature. Generated, usable excess heat and its maximised temperature is compared to a thermal load profile of the district heating network at each moment specifically for a resulting supply energy. The chosen heating network is hereby geographically close to the system in the north-east of Austria.

Moreover, the simulation itself is kept simple with no optimization regarding the fluctuating energy market and a simple straightforward hydrogen and heat production, during times when the grid limit of the power plant is exhausted. The grid limit specifies the maximum power that can be supplied to the electricity network at any given time. For economic considerations in terms of heat, a lump feed-in rate is assumed.

2 Methods

2.1 Scenario(s) and System Overview

To evaluate this system, the scope needs to be defined and justified assumptions need to be made. In this case, the analysed system (visualized in Figure 1) consisted of the following components: a wind park in the north-east of Austria, photovoltaic (PV) modules, an alkaline electrolyser as well as necessary converters and a grid connection. Hereby, this study assesses the impact of PV and electrolyser sizing on a range of KPIs when varying PV and electrolyser capacities. The wind park has a constant size of 16.5 MW, a profile is generated

using *Meteonorm* [14]. Five different PV capacities from 0 to 20 MW and three electrolysers, namely with a nominal power of 2, 4 and 6 MW, are investigated. It is assumed that the renewables primary task is to generate electricity for grid supply, which is limited to 12 MW. Only if, due to the intermittency of these sources, more energy is produced than can be injected into the grid, the surplus of electricity is utilized to power the electrolyser.

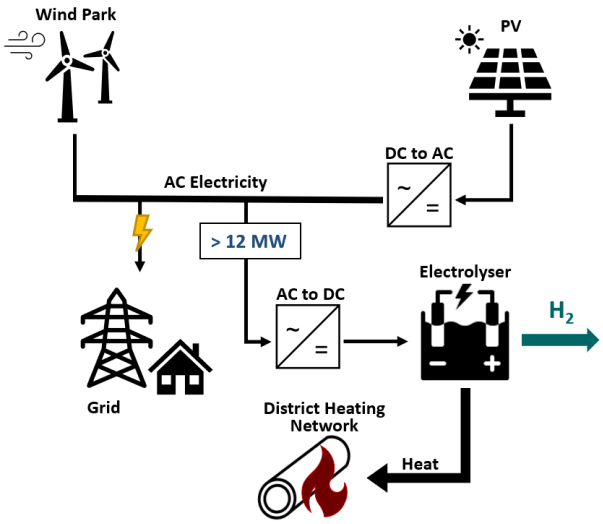

Figure 1: System Boundaries and Visualisation

The electrolyser system itself is organised in serially connected stacks, which consist of individual cells. Additionally, utility equipment essential for operation (pumps, water purification system, ...) is part of the overall electrolyser system. As this study aims to extract useful heat from the electrolyser a heat exchanger is a crucial component as well.

For simulating the chosen system, several input parameters are needed. Besides the basic sizing parameters of PV, wind and electrolyser, additional input parameters and assumptions had to be selected for the newly integrated electrolyser model - these are listed in Table 1.

Parameter	Unit	Value	Source
Operational Temperature	°C	80	[22, 29]
Number of Cells per Stack $\mathbf{N_c}$	-	230	[20, 23]
Stack Power	MW	2.13	[20, 23]
Electrode Area	m^2	2.6	[20, 23]
Stack Lifetime	a	30	[3]
Pressure	bar	6	[16, 29]
Electrolyte	% KOH	30	[16, 29]
Current Density Limit	A/cm^2	0.4	[27]
Stack Thermal Capacity $\mathbf{C_{th}}$	MJ/K	55	[21]
Stack Thermal Resistance $\mathbf{R_{th}}$	K/W	0.004	[21]
Initial Cooling Flow Rate	kg/h	6000	[29]

Table 1: Characteristics of Electrolyser System

2.2 Electrolyser Model

The integrated electrolyser cell model, which is meant to accurately predict the behaviour and output of the electrolyser, is largely based on four literature sources: [2, 25, 29, 30]. It is divided in three main parts: the thermodynamic, the electrochemical and the thermal model.

2.2.1 Thermodynamic Model

First, the goal of the thermodynamic model is to determine the reversible and thermoneutral voltage with the inputs of temperature, pressure and concentration of potassium hydroxide (KOH) in the electrolyte.

First, since the reversible voltage is temperature and pressure dependent a rather complex expression, the Nernst-Equation, is adapted for the model [25, 30]:

$$V_{rev} = V_{rev}^{0} + \frac{RT}{zF} ln\left(\frac{\left(P - P_{v,KOH}\right)^{\frac{3}{2}}}{a_{H_2O,KOH}}\right) \qquad 2.1$$

The first term estimates the reversible voltage $\mathrm{V_{rev}^{0}}$ at a certain temperature, which is determined with an empirical expression. The second part of the equation accounts for the influence of pressure on the reversible potential, which depends on the water vapour pressure $\mathrm{P_{v,KOH}}$ and the water activity $\mathrm{a_{H_2O,KOH}}$ of the KOH solution. The values of these are calculated using empirical expressions listed in [30] that depend on the temperature and pressure independent molality m of the solution. The molality of a solution is the ratio of the number of moles of the solute and the mass of the solvent [26]. Knowing the mass concentration of KOH in the solution as well as the molar mass of KOH [17], the molality can be calculated.

Since the thermoneutral voltage only varies minimally with T and P, the thermoneutral voltage $\mathrm{V_{tn}}$ was kept constant at 1.482 V [29] in this model due to simplicity.

2.2.2 Electrochemical Model

Following the thermodynamic model, the electrochemical model is an integral part of the electrolyser model, as it calculates the cell voltage, the hydrogen output and the corresponding efficiency of the system based on the thermodynamic results, the stack characteristics and the provided current from renewables. The majority of it follows Ulleberg's approach [29].

In a real electrolyser the water splitting process is not ideal, which leads to voltage drops mainly due to slow kinetics at the electrodes and ohmic losses in the electrolyte. Consequently, overvoltages need to be applied to the system to counteract these phenomena: the activation overvoltage $\mathrm{V_{act}}$ and the ohmic overvoltage $\mathrm{V_{ohm}}$, which – together with V_{rev} – add up to the total cell voltage V_{cell}. Often an empirical model is used to determine the relation between voltage and current (*U-I*) or current density (*U-i*). This results in equation 2.2 with *r* as the ohmic resistance parameter and overvoltage coefficients *t* and *s* (values according to [25]).

$$V_{ohm} = (r_1 + r_2 T) \cdot i \quad \text{and} \quad V_{act} = s \cdot ln\left[\left(t_1 + \frac{t_2}{T} + \frac{t_3}{T^2}\right) \cdot i + 1\right] \qquad 2.2$$

In equation 2.3 formulas for relevant efficiencies of the electrolyser are shown. Faraday Efficiency η_F of an electrolyser cell is the ratio between the real hydrogen output and the theoretical one. The losses related to this efficiency are due to parasitic current losses, which

increase with cell voltage. In this case an empirical expression is given [29]. Additionally, electrical losses are represented by the energy efficiency η_e, which depends on the cell voltage. The product of these two efficiencies makes up the total efficiency of an electrolyser without considering auxiliary losses.

$$\eta_F = \frac{i^2}{f_1 + i^2} \cdot f_2 \quad | \quad \eta_e = \frac{V_{tn}}{V_{cell}} \tag{2.3}$$

Faraday's law states that hydrogen generated at the electrode is directly proportional to the current flowing in the electrolyser. As a result, the molar hydrogen flow rate produced, per stack, is determined as follows:

$$\dot{n}_{H_2} = \eta_F \cdot \frac{N_c I}{zF} \tag{2.4}$$

2.2.3 Thermal Model

A thermal model is crucial for an analysis of the generated heat of an electrolyser since the temperature of both the electrolyser and the cooling fluid are estimated and also regulated throughout the simulation. Additionally, various heat instances are calculated with a special focus on the usable thermal energy.

For this model, a lumped thermal capacitance model for the whole electrolyser stack is used, the same as in Ulleberg's [29] and Adibi's [2] approaches. The total heat balance in the electrolyser stack consequently is given as:

$$\dot{Q}_{st} = C_{th} \frac{dT}{dt} = \dot{Q}_{gen} - \dot{Q}_{loss} - \dot{Q}_{exch} - \dot{Q}_{cool} \tag{2.5}$$

Hereby, Q_{st} is the stored energy in the electrolyser, which is the generated heat $\mathrm{Q_{gen}}$ minus heat loss to the ambient $\mathrm{Q_{loss}}$, thermal energy invested in sensible and latent heat transfers $\mathrm{Q_{exch}}$ and cooled heat $\mathrm{Q_{cool}}$. The calculation of these heat variations follows the approach in [29] and [2].

Cooling System Integration

The management and calculation of $\mathrm{Q_{cool}}$ is directly connected to the implementation of the cooling system for the simulation, which is part of the thermal model [2, 29]. Since no additional heating component is part of the overall system, the electrolyser temperature is equal to the ambient temperature at first, which is assumed at 25 °C. So initially, the electrolyser is not cooled and its generated heat is utilized to heat itself up. Once the desired operation temperature is reached, the cooling is activated.

The thermal energy that can be extracted via cooling is estimated using the mass flow of the cooling water $\dot{m}_{CW}$, heat capacity of water C_{p,H_2O} and the temperature difference T_{diff} between in- and out-flowing cooling liquid.

$$\dot{Q}_{cool} = \dot{m}_{CW} C_{p,H_2O} T_{diff} \tag{2.6}$$

For the calculation of $\mathrm{T_{diff}}$, the heat transfer coefficient UA_{HX} of the heat exchanger, specifically the cooling coil, is essential.

$$T_{diff} = (T - T_{CW,in})\left(1 - exp\left(-\frac{UA_{HX}}{\dot{m}_{CW}C_{p,H_2O}}\right)\right) \quad 2.7$$

Subsequently, the new temperatures after a timestep are estimated via the following expressions:

$$T(t) = T(t - \Delta t) + \frac{\Delta t}{C_{th}}Q_{st} \quad \text{and} \quad T_{cool} = T_{CW,in} + T_{diff} \quad 2.8$$

For the electrolyser temperature a relatively simple method has been applied. With the assumption of a constant heat production and thermal energy transfer a quasi steady-state model can be used (equation 2.8).

Since the supply temperature of Austrian District Heating networks needs to be above 65 °C [13], the outlet cooling temperature needs to fulfill these constraints. Therefore, if the electrolyser is cooling, the initial cooling flow rate in a specific timestep is adjusted within the simulation until the cooling water temperature is at least 65 °C. This is possible because a reduced cooling flow rate results in a higher temperature of the fluid, but nevertheless, it can not be decreased too far as reduced cooling flow also translates directly to a decreased amount of thermal energy removed from the system.

2.3 Technical Components and Analysis

2.3.1 Components and Simulation Framework

The utilized simulation tool is organised in components that make up the whole system. Firstly, the electricity suppliers, wind and PV, are each a component of their own. Then converters are needed, to generate AC and DC electricity for grid supply and the electrolyser respectively. Ultimately, the electrolyser is the central component of the system and it is largely constructed as described above.

2.3.2 Integrating Heat into District Heating Network

In order to analyse the potential of integrating the waste heat of an electrolyser into a district heating system, the extracted cooling energy Q_{cool} was compared to a thermal load profile from a District Heating (DH) network [28], which is located geographically close to the Wind Park. The heat demand peaks at 0.9 MW during the winter and is considerably lower around a few hundred kW during the summer. The comparison between both profiles is done timestep by timestep, which is chosen to be 10 min. This also means that if the cooling is deactivated, even momentarily, because no power is fed to the electrolyser, no heat can be supplied to the heating network.

2.3.3 Technical KPIs

To evaluate the technical performance of the system, several KPIs are defined, calculated and determined for each combination of PV and electrolyser capacity for a profound analysis (see Table 2).

KPI	Symbol	Formula	Description
Full Load Hours	-	$\frac{E_{H_2}}{P_{nominal,H_2}}$	Characterises how efficiently the system runs throughout the year
Overall Efficiency	η	$\frac{E_{H_2}}{E_{input}}$	Overall efficiency of the established electrolyser system (including auxiliary losses estimated at 2.5 % of supplied energy [19])
Efficiency considering cooling potential	η_{cool}	$\frac{E_{H_2} + Q_{cool}}{E_{input}}$	Enhanced efficiency regarding theoretically usable cooling output
Efficiency considering DH supply	η_{DH}	$\frac{E_{H_2} + Q_{toDH}}{E_{input}}$	Enhanced Efficiency regarding supplied heat to the DH network
Share of Usable Curtailment Energy	$\epsilon_{curtailed}$	$\frac{E_{H_2} + Q_{toDH}}{E_{curtailed}}$	Percentage of curtailment energy from the renewables that can be repurposed as hydrogen or heat
Fulfilled DH Demand	α_{load}	$\frac{Q_{toDH}}{Q_{load}}$	Share of thermal energy demand that can be fulfilled

Table 2: List of Technical KPIs

2.4 Economic Evaluation

In order to calculate the Levelized Cost of Energy of a system, the relevant capital and operational expenditures (CAPEX and OPEX) need to be defined. Table 3 lists all the CAPEX values that are necessary to determine economic KPIs. The Electrolyser CAPEX hereby includes auxiliary equipment like the water deioniser [20]. The operating costs of the components are assumed to be about 2 % of the CAPEX [1].

Capital Expenditures [€/kW]	
Electrolyser System	750 [15, 20]
AC/DC Converter	150 [10, 11]
Heat Exchanger	90 [24]

Table 3: Relevant CAPEX values

The focus of the economic analysis is the Levelized Cost of Energy. It represents the cost to produce energy within the system over an assumed lifetime. Equation 2.9 shows the expression for determining the levelized cost. Besides CAPEX and OPEX values, also the weighted average cost of capital (wacc) needs to be set and it is estimated to be 6 % [7].

$$LCOE = \frac{\sum \frac{CAPEX_t + OPEX_t - R_{heat,t}}{(1+wacc)^t}}{\sum \frac{E_t}{(1+wacc)^t}} \qquad 2.9$$

The Levelized Cost of Hydrogen is a measure for determining how competitive the hydrogen price of this system is, compared to other forms of hydrogen production. In this scenario, as the electricity used for the electrolyser is only excess energy from the renewables it is

considered to be free of charge. Therefore, only the expenditures for the electrolyser system itself and the connected AC/DC converter are used for the calculation. In a first step, the LCOH is calculated without considering the revenues from providing heat to the district heating network: R_{heat}= 0. Secondly, the impact of selling heat on the price of hydrogen is investigated for which the potential income from supplying heat to the DH network has to be defined. Based on values found in literature, a pessimistic and an optimistic scenario, at 25 and 40 €/MWh respectively, is defined [8].

An analysis of the Levelized Cost of Heat (LCOHeat) is crucial to determine if it is even feasible for this system to sell the provided thermal energy at the prices listed above. The assumption was made that the electrolyser is built to provide hydrogen first and foremost and consequently, only the expenditures of the additional heat exchanger are considered for LCOHeat.

3 Results and Discussion

3.1 Model Validation

In the polarisation curve of the implemented model and electrolyser stack is shown. Different to standard operation, the pressure was elevated to 16 bars and the KOH concentration in the electrolyte was 25 %. This was done to create a validation for the integrated model as measurement points from Sakas et al. [25] at 70 °C were utilized. Additionally, the reversible voltage of the established system at 6 bar, 30 % KOH and 80 °C is 1.231 V, which is reasonable as V_{rev} at standard conditions (1 bar and 25 °C) is 1.229 V. Pressure as well as electrolyte concentration have the effect of elevating the reversible voltage, while increased temperature decreases it [29].

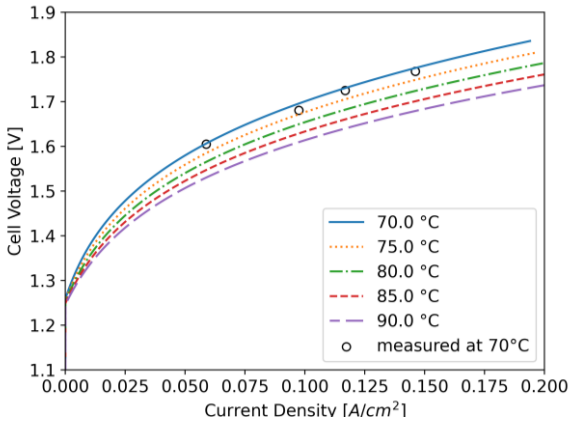

Figure 3: Simulated Polarisation Curve including measurement points from [25]

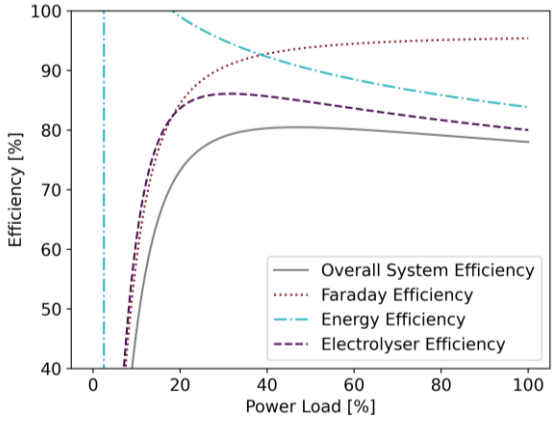

Figure 2: Efficiency of the investigated system at 80 °C

To further validate the implemented electrolyser model, the hydrogen production per hour at maximum power for 1 stack (= 2.13 MW) was determined and compared to Rizwan et al.' and Qi et al.' values [21, 23]. With 480.6 Nm^3/h the result from this simulation is perfectly reasonable for the lower MW electrolyser scales, the direct correlation to the production rate in [23] is especially fitting as the same stack size is utilised in both cases.

The typical efficiency curve of the electrolyser stack is presented in Figure 3. The behaviour of energy and faraday efficiency depending on the power load is visualised and as described in section 4, the product is the Electrolyser Efficiency. The Overall System Efficiency η is the

essential one and the difference to the modelled efficiency originates in the auxiliary losses. The operation of the electrolyser is limited to a minimum of 15 % partial load due to gas contamination [5, 31], which is beneficial when looking at the drop in efficiency below roughly 20 %. Moreover, the efficiency of the electrolyser peaks at around 25-30 %, but afterwards it does not decrease significantly either, which is favorable for regular operation.

3.2 Seasonal Simulation Analysis

In order to analyse the operation of the electrolyser more detailed, a seasonal insight into the simulation step-by-step is given in Figure 4. For the following examples, a PV capacity of 5 MW and a single electrolyser stack was selected (16.5 MW wind and 12 MW grid limit). It is noticeable that there is a tendency for less hydrogen production during the colder months of the year, which is in correlation to the solar-powered electricity production. The middle plot visualises the temperature profile of both the cooling liquid and the electrolyser. The cooling liquid is always at 14.5 °C before the cooling process, which aids the visualisation of an (in)active cooling system in the graphic. At nominal power, largely presented in the autumn graphic, the temperature stays constant at approximately 80 °C, while it shows small variations, when the power is not constant as can be seen in the middle of summer. Additionally, the heat profile is shown in the bottom plot of the three displayed, where Q_{lost} entails both the heat lost to the ambient and exchange heat. At beginning of an operation phase for the electrolyser, as seen in the two top graphics, the generated heat peaks first, while the cooling is not yet activated. What follows is an increase in operational temperature due to this stored heat and only once the desired temperature setpoint is reached, the cooling starts.

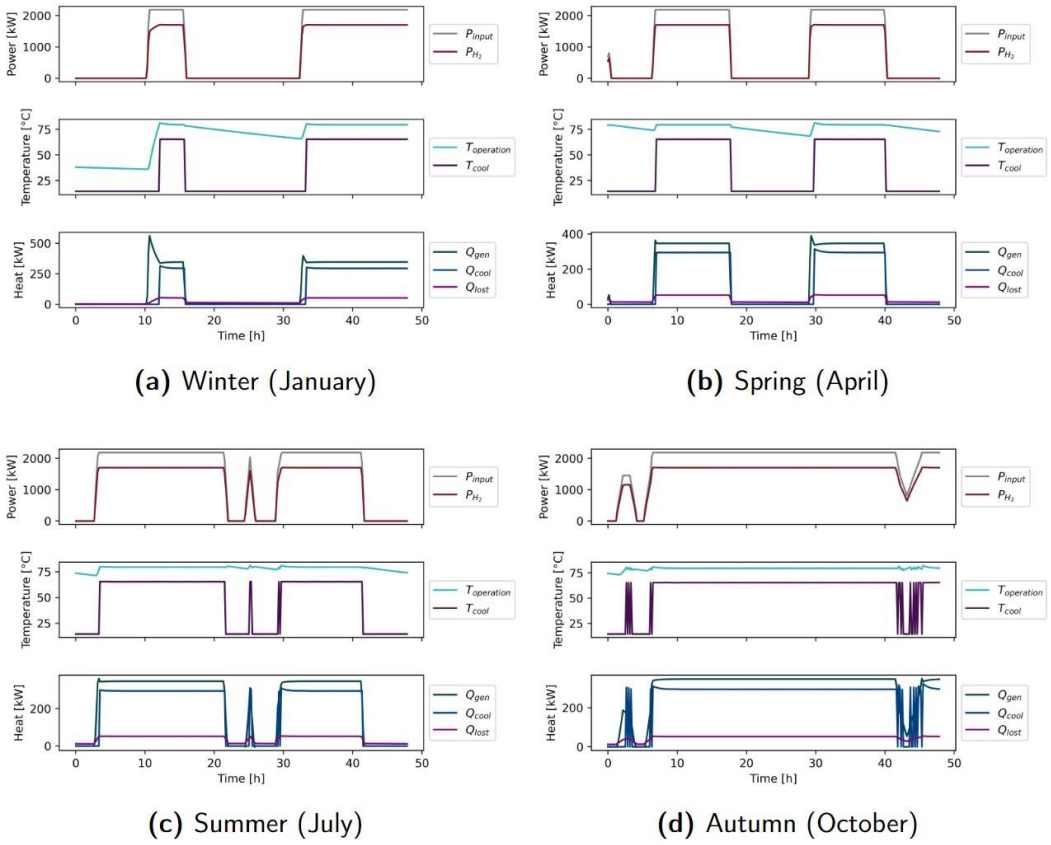

Figure 4: Typical results of selected parameters for different seasons of the year

3.3 KPI Results

3.3.1 Impact Evaluation of PV and Electrolyser Capacity

Figure 5 shows the dependency of three KPIs on PV and electrolyser size. The first one is η_{cool}, which considers the electrolyser's excess heat and is highest for a single stack system. The choice of PV capacity, added to the fixed wind park size, does not seem to have a big impact on this parameter, although it becomes more important with increasing electrolyser size. Due to a simplified cooling strategy at non-nominal and fluctuating electrolyser loads (best seen in the autumn plot), the efficiency including the cooling potential is comparatively quite low for a 6.39 MW system. The bigger the electrolyser the fewer consecutive hours at nominal power can be observed. In general, the efficiency for a single electrolyser stack can be enhanced by about 12 % points if all the extracted heat were to be utilized compared to an electrolyser only producing hydrogen.

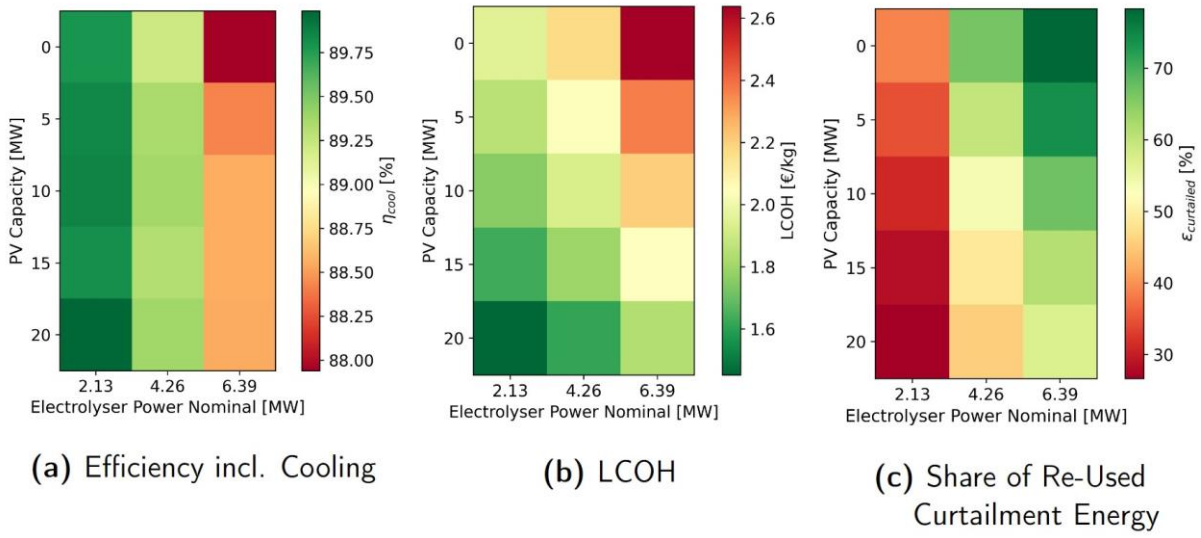

Figure 5: Analyses of KPIs depending on the combination of PV and electrolyser capacity

The LCOH calculations without considering selling heat are presented in the middle graphic and portray hydrogen costs between 1.5 and 2.6 €/kg, which is relatively low and presumably due to the fact that it is assumed that there are no additional costs for the used electricity in this scenario. According to a report from *IEA* in 2021, the cheapest hydrogen prices from fossil fuels are between 0.5 and 1.7 $/kg [12]. Consequently, the cheapest price from this report has the potential to compete with non-sustainable hydrogen prices. The LCOH heatmap additionally shows that a higher PV capacity is beneficial for the price, while more stacks result in a higher LCOH. This is directly correlated to the full load hours of the electrolyser system. Due to the grid limit, more renewable production brings surplus energy to the AEL and a bigger electrolyser requires more energy to operate at nominal power. For a 5 MW PV and single stack system the electrolyser full load hours are equal to roughly 1820 h on average per year.

Since the electrolyser only operates, when there is excess renewable energy, it is additionally relevant to know, which percentage of the otherwise curtailed electricity can be converted to usable energy, namely hydrogen and heat. This is a value that, as can be seen in heatmap to the right, is below 50 % for a single stack system, but rises to almost 80 % with more. An increased PV capacity results in a lower share of re-used curtailment.

3.3.2 District Heating Demand Influence

One of the analysed KPIs was the efficiency in regard to heat supplied to the DH network. In short, η_{DH} for a single stack is approximately 88.2 %, which is lower by about 1.6 percentage points than η_{cool}. This percentage gets worse with higher electrolyser capacity, which can be seen in Table 4. The DH demand using a single stack can be fulfilled to about 15.4 %, when it is connected to a 5 MW PV plant in addition to the wind park. This number rises considerably with higher renewable capacity, but also an increased stack number is at an advantage. It is contradictory that α_{load} is lowest for the biggest electrolyser, but this is a result of the simplified cooling strategy.

	Electrolyser Capacity		
	1 Stack	2 Stacks	3 Stacks
η_{cool} [%]	89.9	89.4	88.4
η_{DH} [%]	88.2	84.7	82.3
α_{load} [%]	15.4	18.5	14.1

Table 4: Technical KPI Results in connection to DH network for 5 MW PV; 1 stack = 2.13 MW

3.3.3 LCOH Reduction with Heat Revenues

As explained before, the LCOH is also calculated considering the profit from the heat sales. In Figure 6 the results for the 5 MW PV scenario are displayed and compared to the original Levelized Cost of Hydrogen. The graphic shows that the improvement is only moderate, the maximum improvement is 11.4 % for one stack in the optimistic case and the minimum enhancement is only 1.8 % for the pessimistic scenario for three stacks. The tendency is therefore towards a lower price reduction with increasing electrolyser size, although increased renewable production can enlarge the relative improvement of the hydrogen price. The total LCOH values are listed in Table 5.

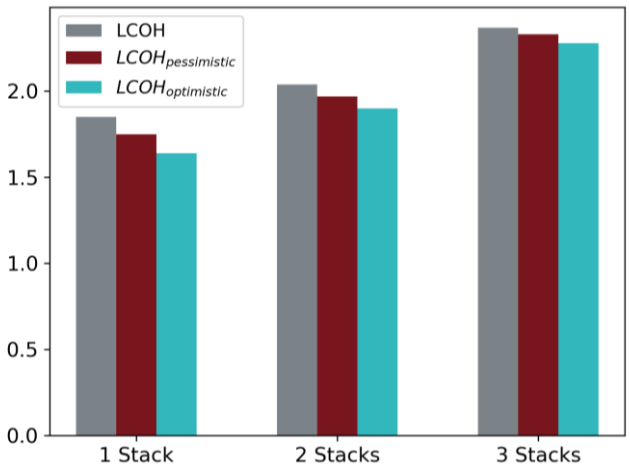

Figure 6: Improvement of LCOH considering optimistic and pessimistic heat revenues

	Electrolyser Capacity		
	1 Stack	**2 Stacks**	**3 Stacks**
$LCOH_{optimistic}$ [€/kg]	1.6	1.9	2.3
$LCOH_{pessimistic}$ [€/kg]	1.7	2.0	2.3
LCOHeat [€/MWh]	8.8	15.6	31.4

Table 5: Economic KPI Results for 5 MW PV; 1 stack = 2.13 MW

3.3.4 Viability for Heat Supply

It is crucial to verify if it is feasible to sell heat, especially in the case of no major LCOH improvement. The resulting LCOHeat is considerably below the pessimistic heat selling price for one or two stacks in the case of 5 MW PV – see Table 5. The LCOHeat for three stacks is considerably higher and even results in a non-viable heat sale in an optimistic case for lower PV capacities. However, the simplified cooling mechanism has to be considered, which has a big impact on the sold heat amount for the biggest system.

4 Conclusion

In this project work, a simulation-based techno-economic analysis of an alkaline electrolyser powered by excess energy from renewables has been executed. A possible utilization of the electrolyser's excess heat and resulting effects on the technical performance as well as the hydrogen price were investigated. For the simulation, an electrolyser model including heat extraction from the system has been implemented and verified against literature values.

The polarisation curve of the integrated electrolyser model aligns reasonably with existing experimental data, affirming its accuracy. Further validation, involving a comparison of hydrogen production rates and a justification of efficiency curves, supports the MW-scale of electrolyser operation.

Regarding the heat generation during electrolysis and the cooling system, a peak in heat generation within the electrolyser is observed at the beginning of an operational period due to initial temperature levels. This is used to heat up the electrolyser and once the desired temperature is reached, the cooling mechanism is activated. However, issues in regard to the simplified cooling strategy are revealed as well with an oscillating cooling system during non-consistent and partial load operation.

The largest (3 stack) electrolyser system is most affected by these problems, as it shows large periods where the electrolyser cannot operate at its nominal power. This affects all KPIs related to the heat output.

Results show that a bigger electrolyser system leads to a slightly reduced efficiency including the cooling potential and increased LCOH, while a higher PV capacity supports a lower LCOH and better fulfillment of the DH demand profile. For one of the most promising scenarios of the study (5 MW PV and one electrolyser stack) - the efficiency is enhanced by over 10 % points with heat provision, while the LCOH is 1.6 €/kg in an optimistic heat sale scenario.

The effect of selling heat only results in marginally improved LCOH values: For the optimal single stack system only around 11.4 % improvement can be achieved and this change in price

varies greatly with stack number and renewable capacity. The analysis further indicates a good economic basis for heat sales with one or two electrolyser stacks, whereas the viability diminishes for larger electrolyser configurations.

These results indicate that an electrolyser powered by surplus renewable energy has future potential in heat and hydrogen generation under the right conditions. Simultaneously, the analysis motivates a closer examination of the cooling mechanism. To additionally improve the synergy with district heating, the consideration of some form of heat storage could pay off due to high heat demand during winters.

5 References

[1] Adam Christensen. 2020. *Assessment of Hydrogen Production Costs from Electrolysis: United States and Europe*. https://theicct.org/wp-content/uploads/2021/06/final_icct2020_assessment_of-_hydrogen_production_costs-v2.pdf. Accessed 19 November 2023.

[2] Adibi, T., Sojoudi, A., and Saha, S. C. 2022. Modeling of thermal performance of a commercial alkaline electrolyzer supplied with various electrical currents. *International Journal of Thermofluids* 13, 100126.

[3] Ansar, A. S., Gago, A. S., Razmjooei, F., Reißner, R., Xu, Z., and Friedrich, K. A. 2022. Alkaline electrolysis—status and prospects. In *Electrochemical Power Sources: Fundamentals, Systems, and Applications*. Elsevier, 165–198. DOI=10.1016/B978-0-12-819424-9.00004-5.

[4] Böhm, H., Moser, S., Puschnigg, S., and Zauner, A. 2021. Power-to-hydrogen & district heating: Technology-based and infrastructure-oriented analysis of (future) sector coupling potentials. *International Journal of Hydrogen Energy* 46, 63, 31938–31951.

[5] Brauns, J. and Turek, T. 2022. Experimental evaluation of dynamic operating concepts for alkaline water electrolyzers powered by renewable energy. *Electrochimica Acta* 404, 139715.

[6] Burrin, D., Roy, S., Roskilly, A. P., and Smallbone, A. 2021. A combined heat and green hydrogen (CHH) generator integrated with a heat network. *Energy Conversion and Management* 246, 114686.

[7] Coppitters, D., Paepe, W. de, and Contino, F. 2020. Robust design optimization and stochastic performance analysis of a grid-connected photovoltaic system with battery storage and hydrogen storage. *Energy* 213, 118798.

[8] DI Gerhard Bucar, DI Karin Schweyer, Ing. Christian Fink, Ing. Richard Riva, DI Michael Neuhäuser, DI Ernst Meissner, Ao. Univ.Prof. Wolfgang Streicher, Christian Halmdienst. 2005. *Dezentrale erneuerbare Energie für bestehende Fernwärmenetze*. https://www.nachhaltigwirtschaften.at/resources/edz_pdf/0678_dezentrale_energieerzeugung_fuer_fernwaerme.pdf. Accessed 27 October 2023.

[9] European Commission. 2020. *A Hydrogen Strategy for a climate neutral Europe*. https://ec.europa.eu/commission/presscorner/api/files/attachment/865942/EU_Hydrogen_Strategy.pdf.pdf. Accessed 6 November 2023.

[10] Fasihi, M., Weiss, R., Savolainen, J., and Breyer, C. 2021. Global potential of green ammonia based on hybrid PV-wind power plants. *Applied Energy* 294, 116170.

[11] Fuchs, N., Jambrich, G., and Brunner, H. 2021. Simulation tool for techno-economic analysis of hybrid ac/dc low voltage distribution grids. In *CIRED 2021 - The 26th International Conference and Exhibition on Electricity Distribution*. Institution of Engineering and Technology, 2549–2553. DOI=10.1049/icp.2021.2122.

[12] IEA. 2021. *Global Hydrogen Review 2021*. https://www.iea.org/reports/global-hydrogen-review-2021. Accessed 20 November 2023.

[13] Köfinger, M., Basciotti, D., Schmidt, R. R., Meissner, E., Doczekal, C., and Giovannini, A. 2016. Low temperature district heating in Austria: Energetic, ecologic and economic comparison of four case studies. *Energy* 110, 95–104.

[14] Meteotest AG. *Meteonorm Software*. https://meteonorm.com/. Accessed 28 November 2023.

[15] Nami, H., Rizvandi, O. B., Chatzichristodoulou, C., Hendriksen, P. V., and Frandsen, H. L. 2022. Techno-economic analysis of current and emerging electrolysis technologies for green hydrogen production. *Energy Conversion and Management* 269, 116162.

[16] Nasser, M., Megahed, T. F., Ookawara, S., and Hassan, H. 2022. A review of water electrolysis-based systems for hydrogen production using hybrid/solar/wind energy systems. *Environmental science and pollution research international* 29, 58, 86994–87018.

[17] National Center for Biotechnology Information. 2023. *PubChem Compound Summary for CID 14797, Potassium Hydroxide*. https://pubchem.ncbi.nlm.nih.gov/compound/Potassium-Hydroxide. Accessed 12 November 2023.

[18] National Research Council and National Academy of Engineering. 2004. *The Hydrogen Economy*. National Academies Press, Washington, D.C.

[19] Parra, D. and Patel, M. K. 2016. Techno-economic implications of the electrolyser technology and size for power-to-gas systems. *International Journal of Hydrogen Energy* 41, 6, 3748–3761.

[20] Proost, J. 2019. State-of-the art CAPEX data for water electrolysers, and their impact on renewable hydrogen price settings. *International Journal of Hydrogen Energy* 44, 9, 4406–4413.

[21] Qi, R., Li, J., Lin, J., Song, Y., Wang, J., Cui, Q., Qiu, Y., Tang, M., and Wang, J. 2023. Thermal modeling and controller design of an alkaline electrolysis system under dynamic operating conditions. *Applied Energy* 332, 120551.

[22] Reuter, S. and Schmidt, R.-R. 2022. Assessment of the Future Waste Heat Potential from Electrolysers and its Utilisation in District Heating. In *NEFI Conference Proceedings*, 54–64.

[23] Rizwan, M., Alstad, V., and Jäschke, J. 2021. Design considerations for industrial water electrolyzer plants. *International Journal of Hydrogen Energy* 46, 75, 37120–37136.

[24] Saini, P., Huang, P., fiedler, F., Volkova, A., and Zhang, X. 2023. Techno-economic analysis of a 5th generation district heating system using thermo-hydraulic model: A multi-objective analysis for a case study in heating dominated climate. *Energy and Buildings* 296, 113347.

[25] Sakas, G., Ibáñez-Rioja, A., Ruuskanen, V., Kosonen, A., Ahola, J., and Bergmann, O. 2022. Dynamic energy and mass balance model for an industrial alkaline water electrolyzer plant process. *International Journal of Hydrogen Energy* 47, 7, 4328–4345.

[26] Shaker, F. N., Obed, A. A., and Abid, A. J. 2023. Practical study on potassium hydroxide molality effect on alkaline electrolyzer HHO production. In *the fourth scientific conference for electrical engineering techniques research (EETR2022)*. AIP Conference Proceedings. AIP Publishing, 50004. DOI=10.1063/5.0155325.

[27] Shiva Kumar, S. and Himabindu, V. 2019. Hydrogen production by PEM water electrolysis – A review. *Materials Science for Energy Technologies* 2, 3, 442–454.

[28] Simon Pezzutto, Stefano Zambotti, Silvia Croce, Pietro Zambelli, Giulia Garegnani, Chiara Scaramuzzino, Ramón Pascual Pascuas, Alyona Zubaryeva, Franziska Haas, Dagmar Exner (EURAC), Andreas Müller (e-think), Michael Hartner (TUW), Tobias Fleiter, Anna-Lena Klingler, Matthias Kühnbach, Pia Manz, Simon Marwitz, Matthias Rehfeldt, Jan Steinbach, Eftim Popovski (Fraunhofer ISI) Reviewed by Lukas Kranzl, Sara Fritz. 2018. *Hotmaps Project*. *D2.3 WP2 Report – Open Data Set for the EU28*. www.hotmaps-project.eu. Accessed 28 November 2023.

[29] Ulleberg, O. 2003. Modeling of advanced alkaline electrolyzers: a system simulation approach. *International Journal of Hydrogen Energy* 28, 1, 21–33.

[30] Ursúa, A. and Sanchis, P. 2012. Static–dynamic modelling of the electrical behaviour of a commercial advanced alkaline water electrolyser. *International Journal of Hydrogen Energy* 37, 24, 18598–18614.

[31] Varela, C., Mostafa, M., and Zondervan, E. 2021. Modeling alkaline water electrolysis for power-to-x applications: A scheduling approach. *International Journal of Hydrogen Energy* 46, 14, 9303–9313.